Md. Ahsan Halimi, Taimoor Khan, Nasimuddin, Ahmed A. Kishk, and Yahia M.M. Antar

Rectifier Circuits for RF Energy Harvesting and Wireless Power Transfer Applications

Low-power wireless sensors will play a big role in smart city applications. These sensors require a power supply to function. Batteries are not optimal for such numerous sensor networks because of their limited life and need for regular maintenance; hence, they are not a universal solution. RF energy harvesting (RFEH) and wireless power transfer (WPT) techniques have the potential to be a green and sustainable solution for supplying power to various low-power devices by capturing ambient RF energy. The ubiquitous nature of RF energy makes it available to exploit and reutilize in power wireless sensor nodes, wireless body area networks, wireless charging systems, RFID tags,

Md. Ahsan Halimi (ahsanhalimi@gmail.com) and Taimoor Khan (ktaimoor@ieee.org) are with the Department of Electronics and Communication Engineering, National Institute of Technology Silchar, Silchar 788010, India. Nasimuddin (nasimuddin@i2r.a-star.edu.sg) is with the Institute for Infocomm Research Singapore, Agency for Science, Technology, and Research, 138632 Singapore. Ahmed A. Kishk (kishk@encs.concordia.ca) is with the Department of Electrical and Computer Engineering, Concordia University, Montréal, QC H3G 1M8, Canada. Yahia M.M. Antar (antar-y@rmc.ca) is with the Department of Electrical and Computer Engineering, Royal Military College of Canada, Kingston, ON K7K 7B4 Canada, and also with Queen's University, Kingston, ON K7L 3N6 Canada.

Digital Object Identifier 10.1109/MMM.2022.3211594

Date of current version: 1 December 2022

©SHUTTERSTOCK.COM/METAMORWORKS

and the Internet of Things [1], [2]. Figure 1(a) displays a conceptual diagram of an RFEH/WPT system. To capture power from free space that is transmitted by the base station, the harvesting node needs a receiving antenna and rectifier to convert the power into dc signals. This dc output is then further utilized to feed a low-power device. Figure 1(b) shows that at 10-m distance from the cellular tower, a digital batteryless watch was powered by a rectenna operating at 1.8 GHz. This LCD watch (low-power device) required 1.5 V to function and was successfully powered up using the RFEH system [3].

To convert received RF energy into a dc signal, the rectifier plays a crucial role in the RFEH/WPT system. Various single-band rectifiers operating in the ultrahigh-frequency (UHF) band, 1.8-GHz band, 2.45-GHz band, 5.8-GHz band, millimeter-waveband, and some other frequencies have been discussed in the existing literature, with the aim of increasing the RF-to-dc power conversion efficiency (PCE). To increase the amount of output dc power, various multiband and broadband rectifiers (BBRs) have been designed [4], [5]. But the ambient electromagnetic (EM) energy in the environment is unpredictable, and so the performance of the rectifier can degrade due to fluctuations in the input power. To minimize the effect of input power fluctuation, a variety of techniques have been adopted for designing rectifiers [6]. This review article focuses on the state-of-the-art classification of rectifiers based on operating conditions, i.e., based on the operating frequency as single band, multiband, and broadband, and based on the operating power level as the low/high power, wide dynamic, and wide incident angle of incoming waves.

Rectification Principle

The output of the diode after the rectification process consists of a dc component as well as fundamental and higher-order harmonics. This is because of the nonlinearity behavior of the diode. According to the Shockley diode equation, the diode current (I_d) can be written as (1):

$$I_d = I_s(e^{cV_d} - 1) \tag{1}$$

where the term c is a constant ($c = q/nkT$), I_s is the reverse saturation current, V_d is the voltage across the diode, q is the charge of the electron, n is the emission coefficient, k

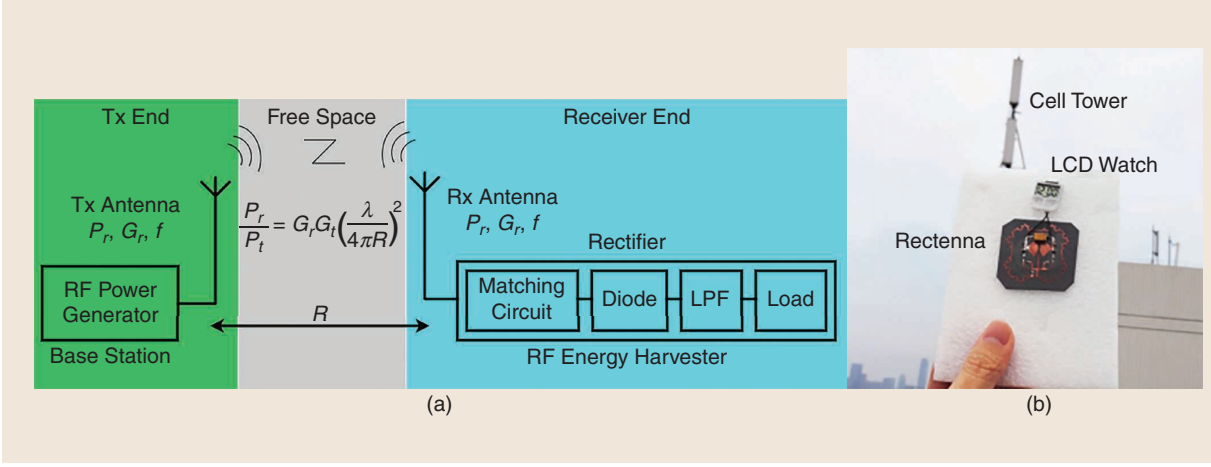

Figure 1. *The (a) wireless energy harvester [6] and (b) application of wireless energy harvesting from a cell tower to power a battery-free LCD watch [3]. Tx: transmitter; Rx: receiver; LPF: low-pass filter.*

is the Boltzmann constant, and T is the absolute temperature. After expanding the preceding equation by applying the Taylor series, the diode current will become

$$I_d = cI_s V_d + \frac{c^2 I_s V_d^2}{2!} + \frac{c^3 I_s V_d^3}{3!} + \frac{c^4 I_s V_d^4}{4!} + \cdots. \quad (2)$$

In an RF energy harvester, the input power of the rectifier is an EM wave supplied by the receiving antenna. Let us consider the voltage across the diode in a sinusoidal form with zero phase shifts:

$$V_d = V_0 \cos(\omega t). \quad (3)$$

By putting the value of V_d from (3) into (2), the diode current will express as

$$I_d = cI_s V_0 \cos(\omega t) + \frac{c^2 I_s V_0^2}{2!}\cos^2(\omega t) + \frac{c^3 I_s V_0^3}{3!}\cos^3(\omega t) + \frac{c^4 I_s V_0^4}{4!}\cos^4(\omega t) + \cdots. \quad (4)$$

After applying the trigonometric rule and arranging it according to the wave pattern, the bias current I_d is expressed as

$$I_d = \left(\frac{c^2 I_s V_0^2}{2.2!} + \frac{c^4 I_s V_0^4}{8.4!}\right) + \left(cI_s V_0 + \frac{c^3 I_s V_0^3}{4.2!}\right)\cos(\omega t) + \left(\frac{c^2 I_s V_0^2}{2.2!} + \frac{c^4 I_s V_0^4}{2.4!}\right)\cos(2\omega t) + \cdots. \quad (5)$$

Equation (5) shows the signal components in the diode current. This can be verified using a spectrum analyzer. Hence, to block the frequency component for good rectification, an RF filter is needed. Also, a large smoothing capacitor working as a low-pass filter or dc pass filter is required to overcome the pulsating nature (ripple) of the output voltage [7].

Classification of Rectifier Circuits for RFEH/WPT

Rectifying circuits embrace diode(s) with and without capacitor(s) based on the topologies involved in the rectifying process. To smooth the output voltage as well as to remove the fundamental and harmonic frequency components from the load, a dc pass filter is needed before the load [8]. A schematic of a rectifier circuit is shown in Figure 2. To increase the dc output power at a particular input power level, it is necessary to maximize the PCE of the rectifier. This requires the proper selection of both the diode and the rectifier typology, depending upon the available input power level [6]. There are four different criteria that can be used to classify rectifiers, as demonstrated in Figure 3. Based on the nonlinear device, the devices can be classified as diode-based rectifiers and MOS-based rectifiers. Based on the topology, they can be

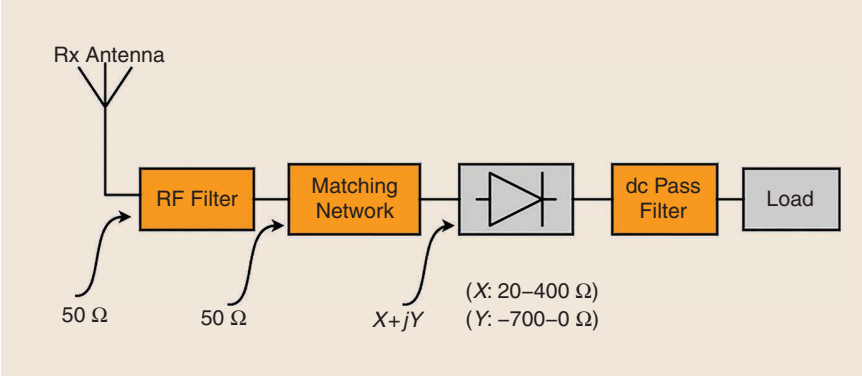

Figure 2. *The rectifying circuit [9].*

classified as series rectifiers, shunt rectifiers, voltage doubler (VD) rectifiers, and various charge pumps (or voltage multipliers). Based on the operating frequency, they can be classified as single-band rectifiers, multiband rectifiers, and BBRs, whereas based on the operating power level, they can be classified as low/high-power rectifiers, wide dynamic rectifiers, and rectifiers with a wide incident angle of incoming waves.

Classification Based on Operating Frequency

Single-Band Rectifiers

There are several frequency bands that are available to exploit for RFEH/WPT. To exploit the available frequency bands to harvest energy, some rectennas need specific single-band rectifiers operating at the same frequency of interest as that of the receiving antenna. The inefficiency of the RFEH system is due to impedance mismatch between the antenna and the rectifier circuits. For maximum power transfer from the antenna to the rectifier, a single-band matching circuit is necessary.

The RFID community primarily uses the UHF rectifier. Differential drive CMOS UHF rectifiers for RFID applications have been designed for low-power rectification [10]. A cross-coupled dual-path CMOS rectifier was presented for a wide input power range in [11]. Also, cross-coupled CMOS rectifiers with reduced reverse leakage have been presented for WPT applications [12]. In [13], a 0.9-GHz rectifier with class F harmonic termination was presented, and an analytical model to calculate the PCE using time-domain analysis was also derived. It is very interesting to know

The ambient electromagnetic energy in the environment is unpredictable, and so the performance of the rectifier can degrade due to fluctuations in the input power.

that UHF rectifier research has mostly focused on the implementation of CMOS technology. This is because of the acceptable price, power handling, miniaturized dimension, and maturity of CMOS. But at microwave frequencies, a Schottky diode is preferred over a CMOS rectifier for reasons of efficiency [4]. In [3], a full-wave Greinacher rectifier operating at 1.8 GHz was designed to power up a battery-free LCD watch.

Due to the worldwide availability of unlicensed Industry, Science, Medicine (ISM) bands, researchers also focus on designing a rectifier that can operate at 2.45 and 5.8 GHz. In [14], a class DE differential CMOS rectifier with a coupled line matching circuit was proposed for a 2.4 GHz-operated WPT system. In [15], a 2.45 GHz-operated rectifier was designed using coupled transmission line (TL) matching. In [16], a 2.45-GHz rectifier [illustrated in Figure 4(a)] with a $\lambda/8$ short-ended TL in series with a shunt diode was proposed. The $\lambda/8$ TL becomes a $\lambda/4$ TL at the second harmonic and acts as a band stop filter, and the short-ended TL inductive effect compensates for the capacitive effect of the diode and enhances the PCE. A $\lambda/4$ TL and shunt capacitor before the load is utilized to function as a dc pass filter.

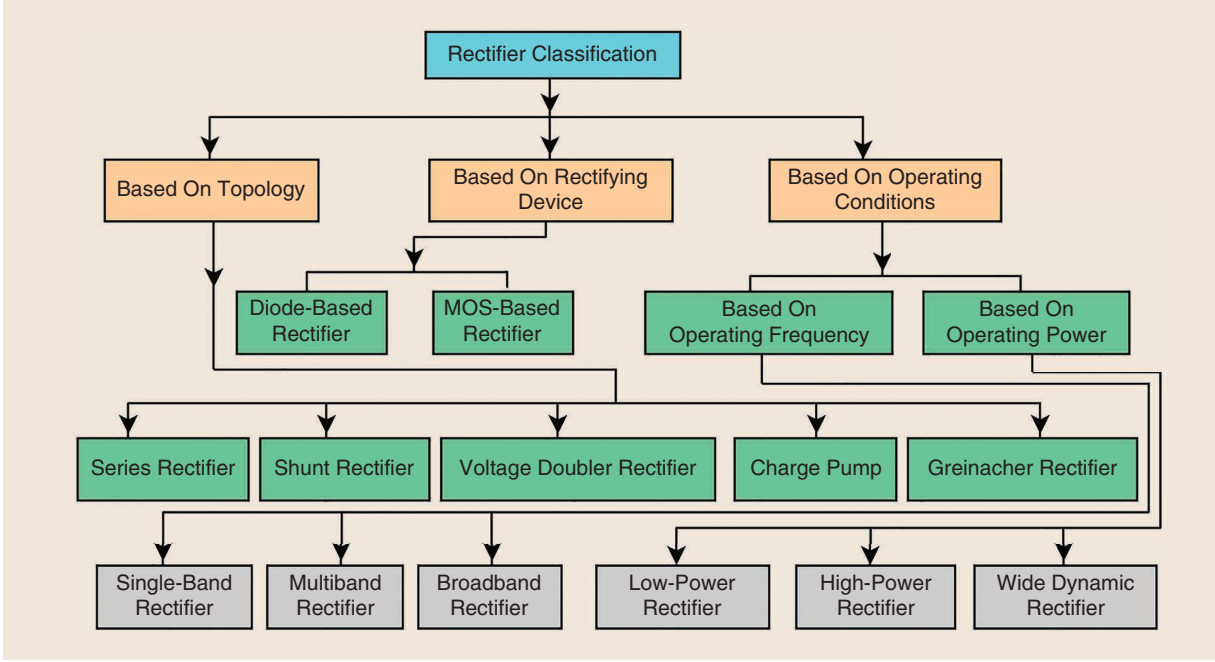

Figure 3. *The rectifier classification.*

In [17], a shunt rectifier was designed using a gallium arsenide (GaAs) Schottky diode to operate at high input power and achieved a 91% PCE at 5 W of input power. In [18], a 2.45-GHz rectifier was designed to handle high input power by using a combination of a GaAs field-effect transistor (FET) and an HSMS-2820 Schottky diode. A watt-level 2.45-GHz rectifier with a class F harmonic termination network (HTN) was demonstrated in [19]. The class F HTN consists of a short-ended $\lambda/12$ TL in series with a shunt diode and open-ended $\lambda/8$ TL for harmonic suppression as well as to cancel the diode parasitic capacitance. However, the 2.45-GHz rectifier was designed to operate at high input power. Some rectifiers that can operate at low input power have been also presented in many kinds of literature. In [20], a 2.45-GHz rectifier with a dual stub matching network (MN) was presented.

Like 2.45 GHz, 5.8 GHz is an ISM band. In [21], a VD rectifier with a class F load and a filter in series with a shunt diode of the VD was designed [as in Figure 4(b)] to enhance the PCE. In [22], a 5.8-GHz rectifier with a class F load to suppress the third harmonic was proposed. In [23], a shunt diode with a single-stub MN was utilized for low-power rectification. In [24], a GaAs Schottky diode in a bridge configuration was utilized to design a 5.8-GHz rectification of high input power. A performance comparison of single-band rectifiers is in Table 1.

Multiband Rectifiers

In the case of wireless energy harvesting (WEH), the amount of available ambient power may be unpredictable and very low. Hence, sometimes single-band WEH systems cannot harvest sufficient power. To increase the harvested power, one of the solutions is to utilize

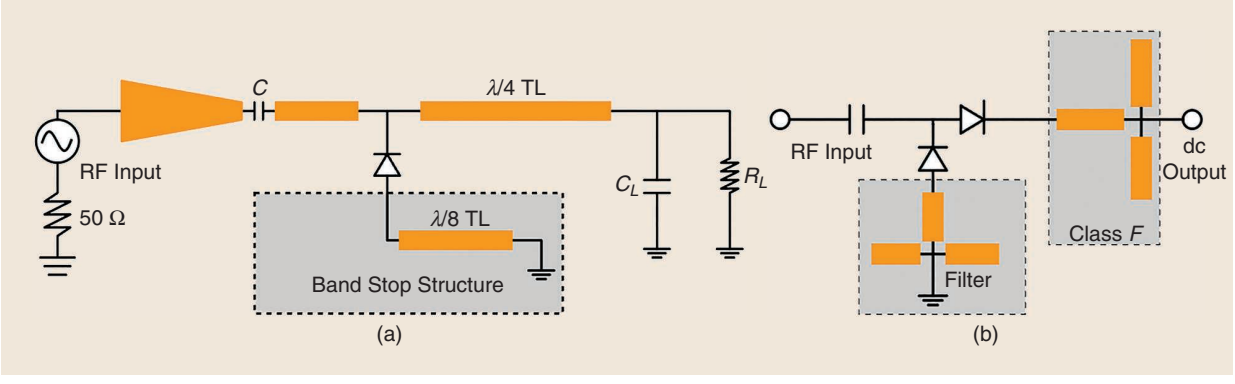

Figure 4. *The single-band rectifier at (a) 2.45 GHz [16] and (b) 5.8 GHz [21].*

TABLE 1. The performance comparison of single-band rectifiers.

Reference	Frequency (GHz)	Rectifier Element and Topology	P_{in} (dBm)	Load (kΩ)	η_{max} (%)
[10]	0.953	0.18-μm CMOS process	−12.5	10	67.5
[11]	0.9	65-nm CMOS process	−10	147	36.5
[12]	0.9	0.18-μm CMOS process	−18.2	100	66
[13]	0.9	HSMS-8202 in shunt	13	0.51	80.4
[3]	1.8	SMS7630 in Greinacher	3	12	65.8
[14]	2.45	65-nm CMOS process	9	0.25	68.5
[15]	2.45	HSMS-2860 shunt	0	4.47	67.7
[16]	2.45	HSMS-282C shunt	20	0.58	80.9
[17]	2.45	GaAs Schottky diode in shunt	37	0.12	91
[18]	2.45	FET with HSMS-2820 in series	30	0.19	74.42
[19]	2.45	HSMS-270B shunt	31	0.115	80
[13]	5.8	MA4E1317 in shunt	13	—	79.5
[21]	5.8	HSMS-2860 VD	14.77	1.7	82
[22]	5.8	HSMS-2860	14.77	1.3	71
[23]	5.8	HSMS-2860	5.75	1.2	72.5
[24]	5.8	GaAs bridge diode	30	0.89	92.8

dBm: decibels relative to 1 mW.

an array of rectennas optimized for different operating frequencies along with a power combiner, as detailed in Figure 5, but this approach makes the system bulky [25]. Another solution is to harvest the energy from more than one source by using a single multiband antenna and multiband rectifier, as shown in Figure 6. There are two methods to design a multiband WEH system. One method is based on a single rectifier with a multiband MN, as presented in Figure 6(a). The second method is based on a stacked rectifier in which each branch has the desired MN, as illustrated in Figure 6(b) [26]. It requires a multibranch rectifier with the desired MN, a power combiner, and a dc pass filter. Hence, multiband rectifier design becomes a challenging and interesting task.

In [27], [28], [29], and [30], dual-band rectifiers utilized a single dual-band MN. A half-wave TL [27], a pair of open- and short-ended stubs [28], a shorted stepped impedance stub composed of two TLs [as in Figure 7(a)] [29], and a T-type MN with a short-ended stub [30] were utilized to achieve dual-band matching. In [31], a dual-band rectifier utilized a two-branch matching circuit, as shown in Figure 7(b). A single triple-band MN was utilized in [26], [32], [33], and

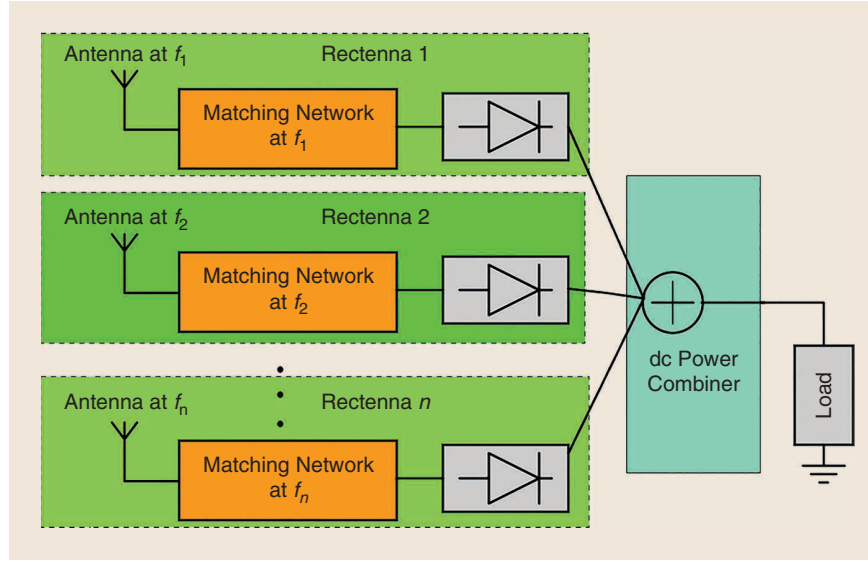

Figure 5. *The rectenna array [25].*

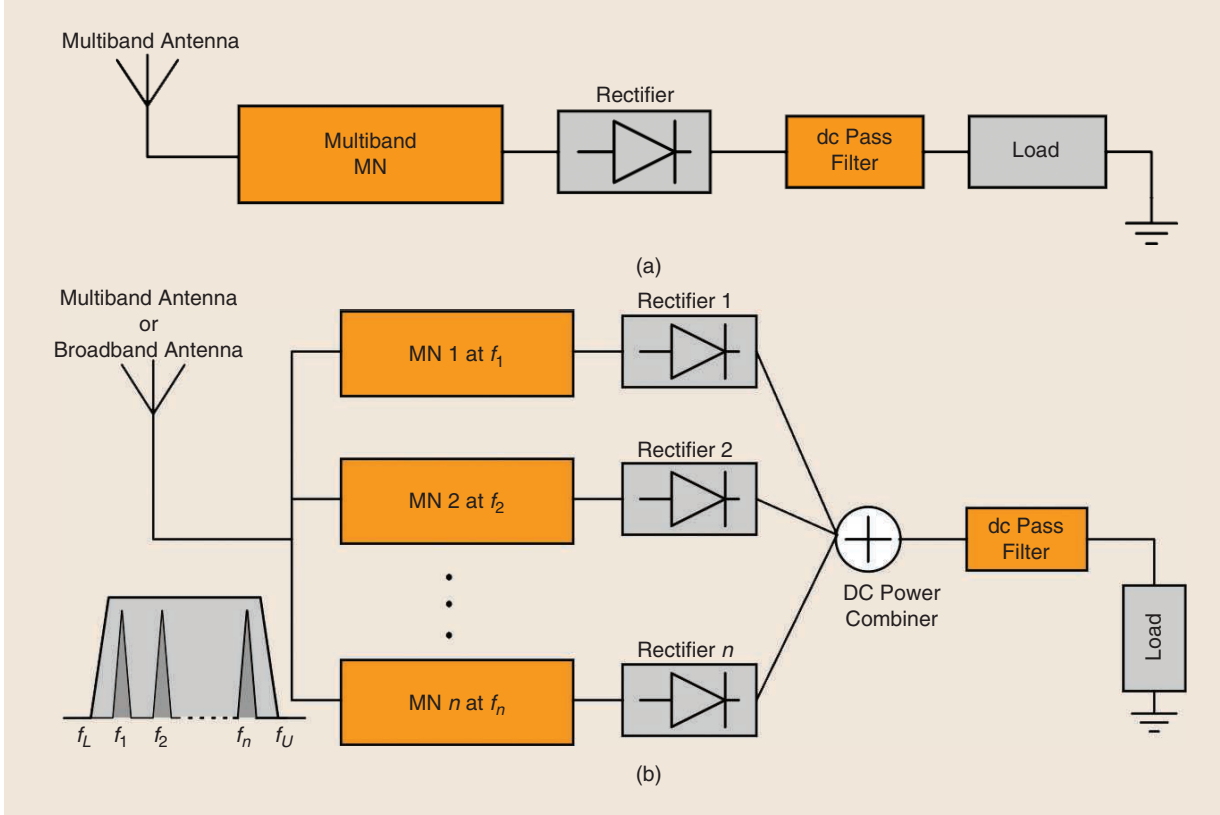

Figure 6. *The multiband rectifier using (a) a multiband MN and (b) a stacked rectifier with the desired matching in each branch [26].*

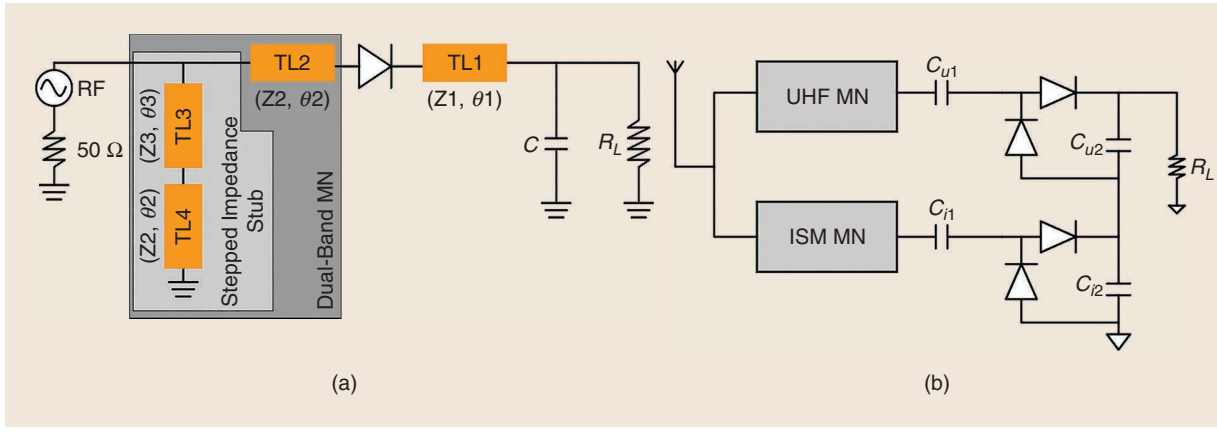

Figure 7. *Dual-band rectifiers using (a) a single dual-band MN [29] and (b) a dual-branch MN [31].*

[34] to design a triple-band rectifier. In [32], a $\lambda/2$ TL and a $\lambda/4$ shorted stub were utilized, and triple-band matching was obtained by tuning its width, as demonstrated in Figure 8(a). In [35], three rectifiers with three different MNs optimized for three different desired frequencies were utilized and combined through a hybrid junction to design a stacked triple-band rectifier, as detailed in Figure 8(b). In [36], a triplexer circuit was utilized to combine the three single-band rectifiers to act as a triple-band rectifier.

In [37], four MNs were designed and placed in a two-stage Dickson to form a quad-band rectifier. In [38], a quad-band rectifier was designed using four stacked branches; each branch was designed in a single band. In [39], a single quad-band MN was utilized to design a quad-band rectifier. A hexa-band rectifier was designed by stacking three cells of a dual-band VD rectifier in [40]. Schematics of quad-band and hexa-band rectifiers are given in Figures 9 and 10, respectively. A performance comparison of multiband rectifiers is in Table 2.

BBRs

A BBR has a task similar to a multiband rectifier, as shown in Figure 11 (i.e., to harvest more power from multiple sources operating inside the desired band). BBR designs are a more challenging task than multiband rectifiers due to the nonlinear rectifying diode. There are theoretical limits to broadband matching over the desired band, as we know from Bode and Fano. Also, it is very difficult to maintain a high PCE in varying operating conditions over a wide bandwidth [6]. In [41], two $\lambda/8$ cross-shaped stubs (one shorted and the other open) were utilized for broadband matching. A T-shaped MN with a $\lambda/8$ open stub [42] and a quasi-T-shaped MN [43] were utilized to achieve broadband impedance matching. A nonuniform TL-based MN was utilized in [44]. In [45], a high-pass-type L section (for lower-band matching) and inductive L section (for upper-band matching) were combined to design a BBR. In [46], a broadband coplanar waveguide rectifier with two series inductive lumped element matching circuits in series with a VD was proposed. Wideband matching based on a coupled line was utilized to design a wideband rectifier of single-series topology in [47]. Other authors have built BBRs by using a harmonic

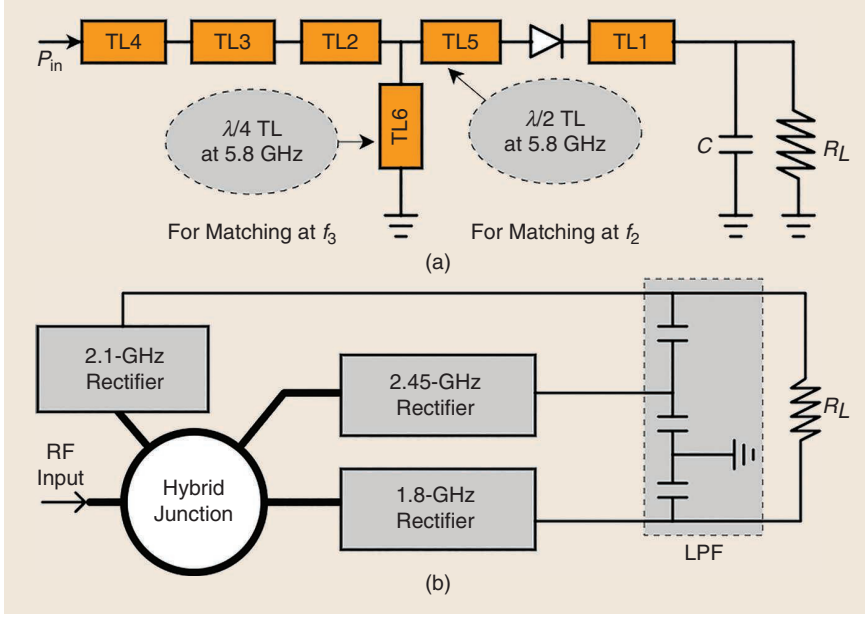

Figure 8. *A triple-band rectifier using (a) a single triple-band MN [32] and (b) a triple-branch MN [35].*

feedback topology [48], multistage TL matching [49], and a frequency selective diode array [50]. Table 3 compares the performance of existing BBRs. Schematics of some BBRs appear in Figure 12.

Classification Based on Operating Power

Low/High-Power Rectifiers

The key component responsible for RF-to-dc power conversion is the Schottky diode used for rectification [51], [52]. The threshold voltage (V_t), breakdown voltage (V_{br}) of the diode, and load influence the performance of the rectifier at particular input power conditions, as detailed in Figure 13 [4], [5], [6]. The sensitivity of the rectifier depends on V_t, while the power handling ability depends on V_{br}. The maximum output voltage ($V_{o\text{Max}}$) and maximum output power ($P_{o\text{Max}}$) can be derived from (6) and (7), respectively:

$$V_{o\text{Max}} = \frac{V_{\text{br}}}{2} \tag{6}$$

$$P_{o\text{Max}} = \frac{V_{\text{br}}^2}{4R_L}. \tag{7}$$

The maximum output power is also inversely proportional to the load resistance (R_L), as shown in (7). Above this power level, the rectifier will break down, and performance will degrade drastically. Hence, the load value also affects the power handling

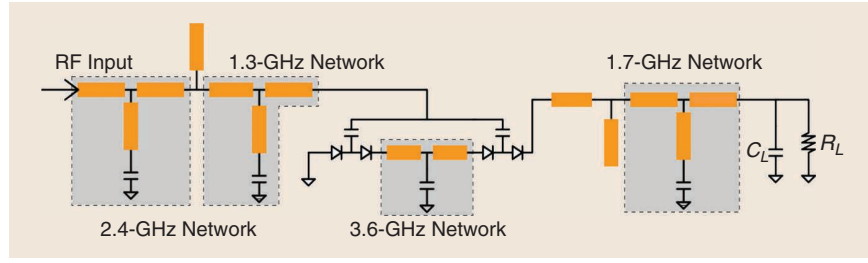

Figure 9. *The quad-band rectifier [37].*

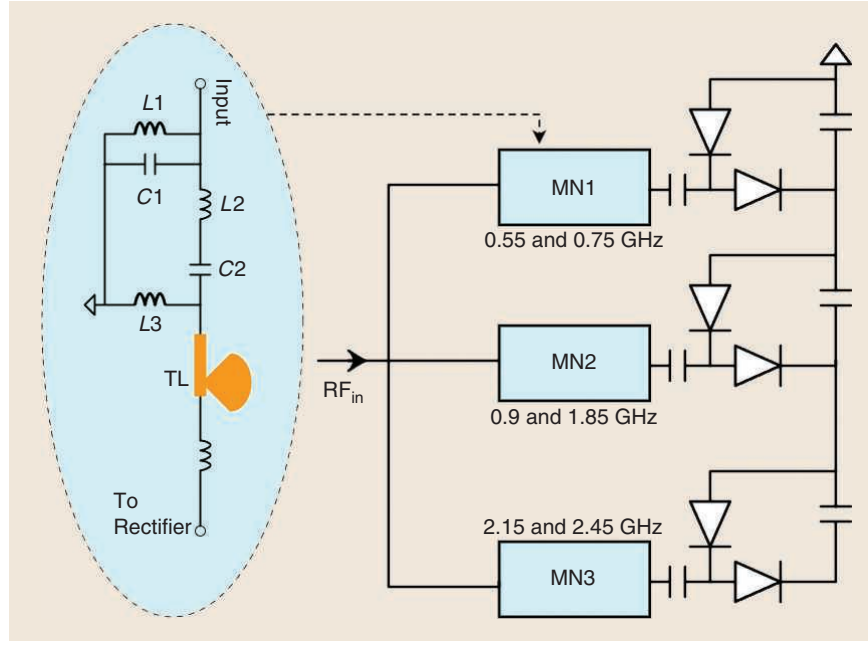

Figure 10. *The hexa-band rectifier [40].*

TABLE 2. The performance comparison of multiband rectifiers.

Reference	Frequency (GHz)	Rectifier Element and Topology	P_{in} (dBm)	Load (kΩ)	η_{max} (%)
[27]	3.5/5.8	HSMS-2860 in series	0	1	51.8/39.7
[29]	0.915/2.45	BAT15-03W in series	9	1.5	74/73
[30]	0.9/2.4	SMS7630 in VD	–1	1.5	69.2/64.1
[26]	1.8/2.1/2.6	HSMS-2850 in series	–20	5.6	35 at triple-tone input
[32]	1.95/2.7/5.8	HSMS-2860 in series	0	2	62.2/59.4/48.9
[33]	24/28/38	MA4E1317 in VD	17.5	1	44/41.3/39.7
[34]	0.85/1.77/2.07	HSMS-2850 in series	0	2.2	61.9/71.5/60.5
[36]	1.85/2.1/2.45	SMS7630 in VD with triplexer	–5	2.7	50 at triple-tone input
[37]	1.3/1.7/2.4/3.6	SMS7630 in Dickson rectifier	0	3	42/40/14/9
[38]	0.9/1.8/2.1/2.4	Metallic MSS20-141 diode in VD	–10	11	63 at multitone input
[39]	0.89/1.27/2.02/2.38	HSMS-2850, HSMS-2860, and FET in series	–10	2	47.8/33.5/49.7/36.2
[40]	0.55/0.75/0.9/1.85/2.15/2.45	SMS7630 in VD in each branch	–5	3.8	80 at six-tone input

The key component responsible for RF-to-dc power conversion is the Schottky diode used for rectification.

capability of the rectifier along with V_{br}. The selection of the Schottky diode based on the operating power level is an important consideration.

A highly sensitive rectifier is needed for a WEH system due to the very low level of ambient power. Figure 13(a) documents that a rectifier with a low threshold voltage works better at low-input-power conditions. Hence, to design a low-power rectifier, a diode with a very low V_t is desirable. The power handling ability depends on V_{br} and the load of the rectifier, as evident in Figure 13(b) and (7). Thus, a diode with a very high V_{br} is better for a high-power rectifier with a low load. The SMS7630 ($V_t = 60 - 120$ mV at 0.1 mA), HSMS-2850 ($V_t = 150$ mV at 0.1 mA), and HSMS-2860 ($V_t = 340$ mV at 1 mA), are best suited for low-power rectifiers due to their low threshold voltage [7], while the HSMS-2820 ($V_{br} = 15\,V$), HSMS-2810 ($V_{br} = 25\,V$) [7], and GaAs Schottky diode $V_{br} = 60$ V) [17] are suitable for high-power rectifiers, due to their large breakdown voltage.

Wide Dynamic Rectifiers

In a real-time WPT system, the location of the receiver (Rx) is not fixed. This results in power level variation due to changes in the Rx position. Similarly, the ambient RF energy is not predictable in an RFEH system. However, the performance of the rectifier in terms of PCE is affected by fluctuations of the input power and variations in the output load [53]. The input impedance of the rectifier may change drastically when there are changes in the input power level and load. This is due to the nonlinear characteristics of the rectifying element (CMOS or diode). Due to this, impedance mismatch will occur and prevent the maximum power transfer. That is why a narrow range of input RF power can convert efficiently into dc power.

Hence, designing a rectifier that is much less sensitive to the input power and load is very important to stabilize performance. Large variations in the input power and load would cause only a small variation in the input impedance of the rectifier. Several

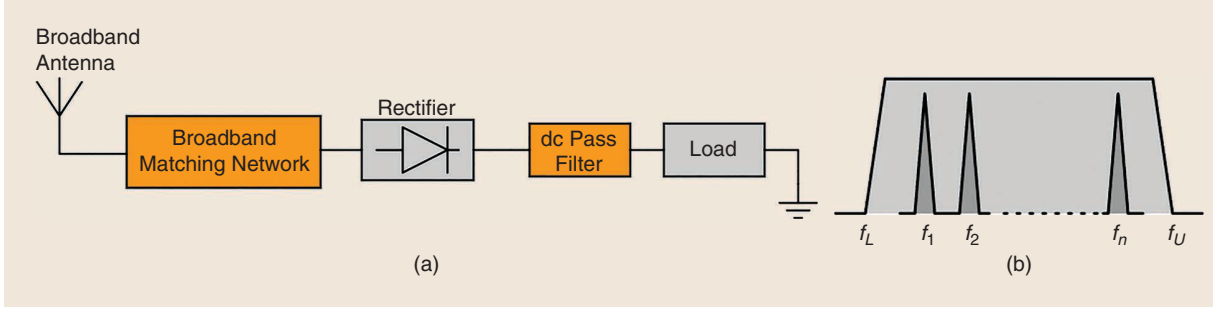

Figure 11. *(a) A BBR [6]. (b) Broadband and multiband spectrum.*

TABLE 3. The performance comparison of BBRs.

Reference	Rectifier Element and Topology	Bandwidth (GHz) at η	η_{max} (%) at P_{in}
[41]	SMS7630 in VD	1–2.05 at >60% at $P_{in} = 8$ dBm	73.2 and 8 dBm at 1.25 GHz*
[42]	BAT-1503W in VD	1–2.7 at >70% at $P_{in} = 15$ dBm	78.2 at 18 dBm at 1.9 GHz
[43]	SMS7630 in VD	0.8–2.45 at >50% at $P_{in} = 8$ dBm	73.1 at 8 dBm at 1.8 GHz*
[44]	SMS7630 in four-diode charge pump	0.47–0.86 at >60% at $P_{in} = 10$ dBm	68 at 10 dBm at 0.55 GHz*
[44]	SMS7630 in two-diode charge pump	0.25–3 at >33% at $P_{in} = 10$ dBm	40 at 10 dBm at 1.5 GHz
[45]	SMS7630 in VD	0.87–2.5 at >30% at $P_{in} = 0$ dBm	63 at 0 dBm at 1.1–1.35 GHz
[46]	SMS7630-005LF in VD	0.1–2.5 at >45% at $P_{in} = 10$ dBm	74.8 at 10 dBm at 1.1 GHz
[47]	HSMS-2860 in series	0.57–0.9 at >70% at $P_{in} = 12.8$ dBm	75 at 15 dBm at 0.7 GHz
[48]	SMS7630 in VD	0.4–2.6 at >40% at $P_{in} = 0$ dBm	64.23 at 8 dBm at 1.4 GHz
[49]	HSMS-2860 in shunt	2–3.05 at >70% at $P_{in} = 10$ dBm	75.8 at 14 dBm at 2.5 GHz
[50]	HSMS-286B array in shunt	1.4–3.7 at >50% at $P_{in} = 10$ dBm	76 at 10 dBm at 1.9 GHz

*Estimated from the graph.

techniques have been adopted to stabilize rectifier performance in dynamic environmental conditions. A resistance compression network (RCN) formed by parallel branches with opposite phase responses can reduce the sensitivity of the rectifier to variations in the input power and load [54]. However, an RCN compresses only the input resistive part. An impedance compression network (ICN) compresses a complex input impedance [55]. Both an RCN and ICN can work under certain impedance conditions with dual-branch topology.

In [56], an integrated ICN was proposed that can operate two parallel diodes in a single branch without any impedance limitations. An approach to extending the operable power is to divide the input power into multiple subrectifier branches that are optimized to operate at different input power ranges. In [57], two subrectifiers (a low-power rectifier and a high-power rectifier) were combined using a T junction power divider. In [58], the rectifier used a branch line coupler (BLC) to add three subrectifiers. Two identical subrectifying branches were utilized for high-power rectification, while the isolation

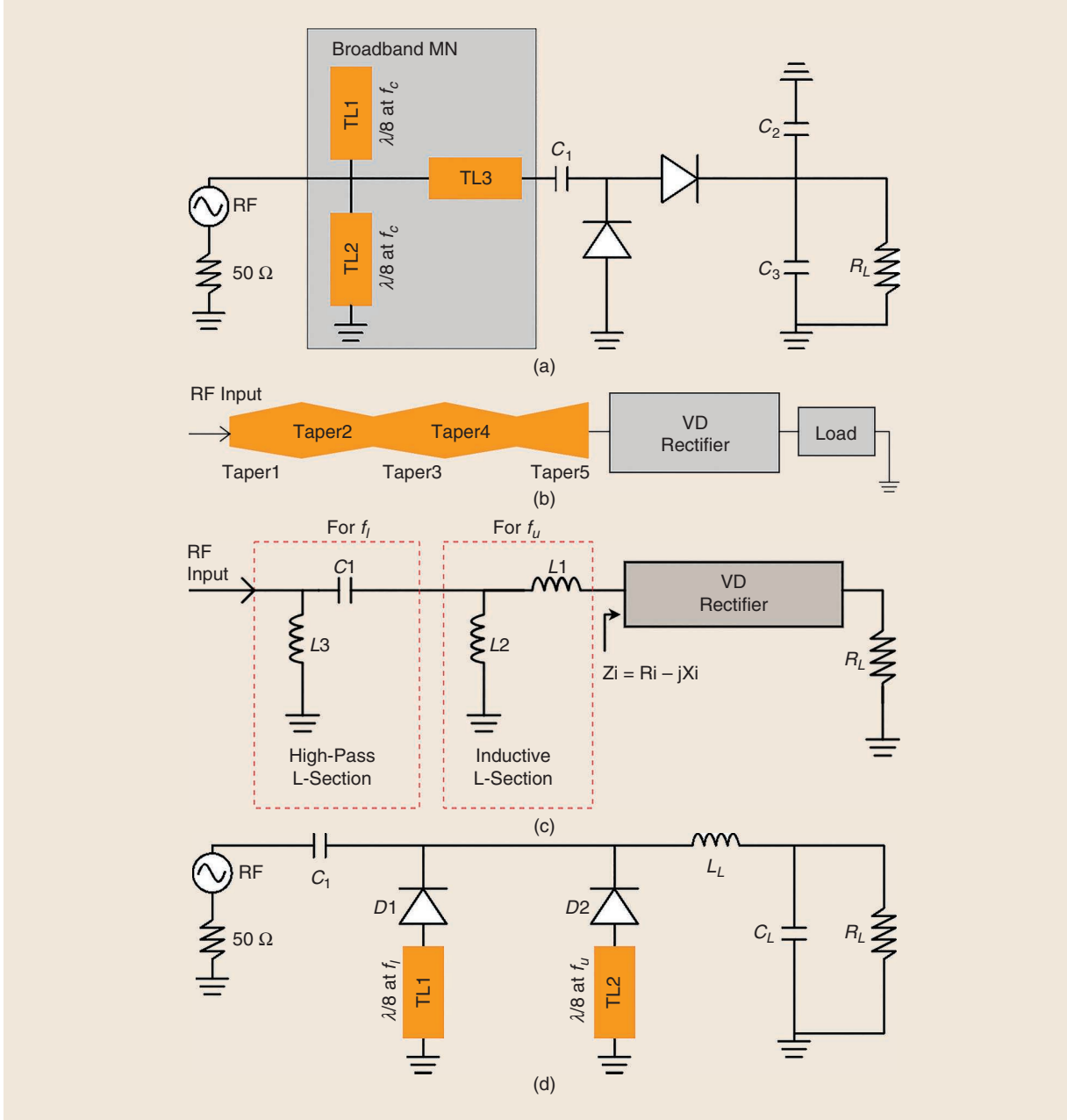

Figure 12. *BBRs designed using (a) dual λ/8 cross-shaped stubs [41], (b) a nonuniform TL MN [44], (c) a high-pass and inductive L section [45], and (d) a frequency selective diode array [50].*

port of the BLC was connected to a low-power subrectifier that collected and recycled the reflected power of the main branch. However, insertion loss due to the extra components, such as the power divider and coupler, was unavoidable, resulting in performance degradation. In [59], the automatic input power distribution technique (AIPDT), employing two segments of the microstrip line, was utilized to adaptively distribute the input power in the subrectifier branch operating at a low- and high-power level. The proposed AIPDT has low loss because it employs only two segments of the microstrip line.

A rectifier array consisting of multiple subrectifiers optimized for different operating power levels with an adaptive power distribution technique has been proposed for a wide operating range of input power. In [60], a power division diode array (PDDA) of two parallel subrectifiers was used to enhance the dynamic power range. In such a rectifier array, the RF input power is distributed among multiple rectifier devices adaptively, according to their impedances as a function of the input power level. An impedance matching circuit using a varactor diode with self-tuning impedance matching (STIM) was proposed to boost immunity to input power fluctuations in [61]. This approach improved the matching and extended the operating power range. The authors of [62] combine the Schottky diode and FET to design a wide-dynamic-range rectifier, while in [63], a pseudomorphic high-electron mobility transistor (pHEMT) is utilized along with the Schottky diode to extend the operating power range. A performance comparison of rectifiers designed to operate over a wide input power range is available in Table 4. Some rectifiers that have been designed to extend the operating power range are depicted in Figure 14.

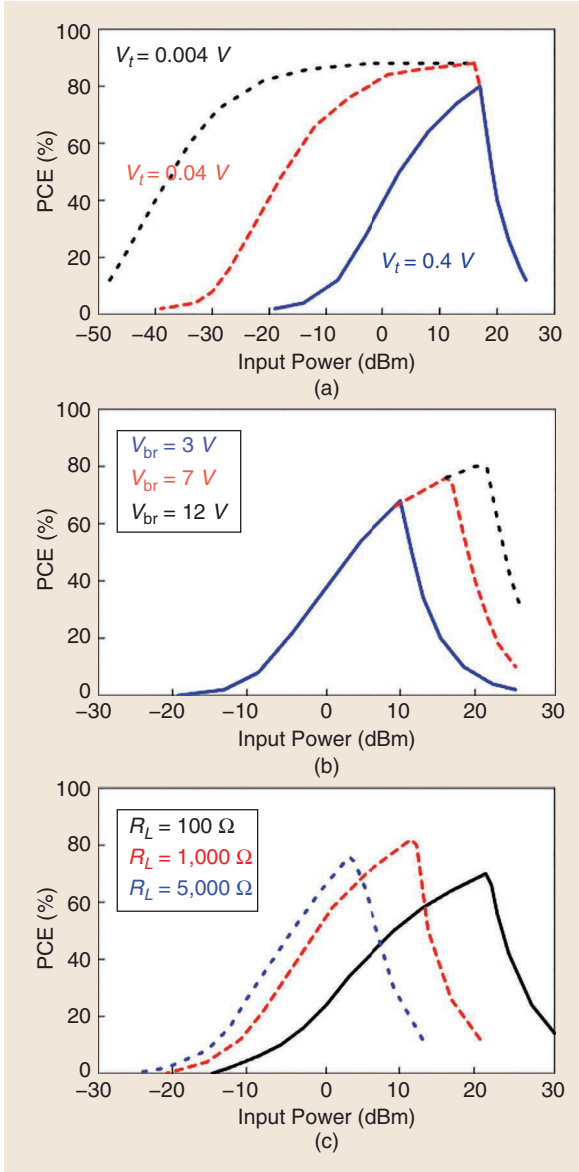

Figure 13. *The effect of (a) V_t, (b) V_{br}, and (c) the load on rectifier performance. dBm: decibels relative to 1 mW.*

Rectifiers With Wide Incident Angle of Incoming Waves

In an RFEH system, the ambient RF energy is unpredictable and very low. To increase the amount of energy, a possible solution is to use multiple antennae with an RF power combiner [as shown in Figure 15(a) for an array of two antennae]. A rectifier is used here to rectify combined RF energy. When the incident wave has a different phase angle (phase difference = $\Delta\varphi$), the PCE of the rectifier will be $0.5(1+\cos(\Delta\varphi))$ times the PCE of the rectifier working in normal conditions. When the phase difference of the two incoming signals is 180°, the efficiency will become zero, as illustrated in Figure 15(b). To overcome this issue, there is a need for a rectifier that is insensitive or less sensitive to the angle of the incident wave. In [64] and [65], a wide-incident-angle rectifier is proposed using a Wilkinson power combiner (WPC), as in Figure 15(c), and subrectifier 1 collects the energy from two ports and finds its maximum PCE at $\Delta\varphi = 0°$, and at this time, the PCE of subrectifier 2 will be zero. When $\Delta\varphi = 180°$, no energy will flow to subrectifier 1; only subrectifier 2 receives all the energy and finds its maximum PCE. For all the other values of $\Delta\varphi$, both rectifiers receive the energy, and the sum of the PCEs maintains the maximum PCE.

The problem with the previously discussed WPC-based rectifier is the performance of the MN. Because the diode is nonlinear, the input impedance of the rectifier varies according to the input power levels. The change in the phase difference changes the input power to the rectifier and, hence, the input impedance, which degrades the PCE of the rectifier. To overcome the impedance mismatch issues that arise in the rectifier based on a WPC, a rat race coupler (RRC) was utilized to design a wide-incident-angle rectifier in [65].

TABLE 4. The performance comparison of rectifiers for wide dynamic range.

Reference	Frequency (GHz)	Rectifier Element and Technique	P_{in} (dBm)	η_{max} (%)	Dynamic Input Power Range
[54]	0.915/2.45	HSMS-2862 and RCN	17	74.9 72.6	20.9 dB (0.3–21.2) at $\eta \geq 50\%$ at 0.915 GHz 13.5 dB (5.1–18.6) at $\eta \geq 50\%$ at 2.45 GHz
[54]	1.8/2.4	HSMS-2862 and RCN	18	75.8 70.9	15.6 dB (4.9–20.5) at $\eta \geq 50\%$ at 1.8 GHz 13.2 dB (6.6–19.8) at $\eta \geq 50\%$ at 2.4 GHz
[55]	2.45	HSMS-286F and ICN	17.8	79.2	13.5 dB (6–19.5) at $\eta \geq 60\%$*
[56]	2.45	HSMS-286F and ICN	14.1	73.6	12.8 dB (4.2–17) at $\eta \geq 60\%$
[57]	0.915	HSMS-2822 and two subrectifiers with T junction	29	68	26.5 dB (4–30.5) at $\eta \geq 50\%$
[57]	0.915/2.45	HSMS-2822, HSMS-2822, and two subrectifiers with T junction	30	66 58	42 dB (–9–33) at $\eta \geq 40\%$ at 0.915 GHz# 21 dB (10–31) at $\eta \geq 40\%$ at 2.45 GHz*
[58]	2.45	HSMS-2820, HSMS-2860, and three subrectifiers with BLC	26.5	62*	24 dB (8.5–32.5) at $\eta \geq 50\%$
[59]	2.4	HSMS-282, HSMS-286, and AIPDT	17	81.2	24.3 dB (2.2–26.5) at $\eta \geq 50\%$
[60]	2.45	HSMS-282 and PDDA	27	74.5	23.3 dB (6.5–29.8) at $\eta \geq 50\%$
[60]	2.45	HSMS-286, HSMS-282, and PDDA	28	68.5	31 dB (–1–30) at $\eta \geq 50\%$
[61]	2.4	HSMS-282B and STIM	20.5	81.2	23 dB (2.5–25.5) at $\eta \geq 50\%$
[62]	1	HSMS-2860, HSMS-2850, and FET	17	80	24 dB (–4–20) at $\eta \geq 50\%$
[63]	0.915/1.8	HSMS-2850 and pHEMT	4	56*	35 dB (–15–20) at $\eta \geq 50\%$ for dual-tone input

*Estimated from the graph.

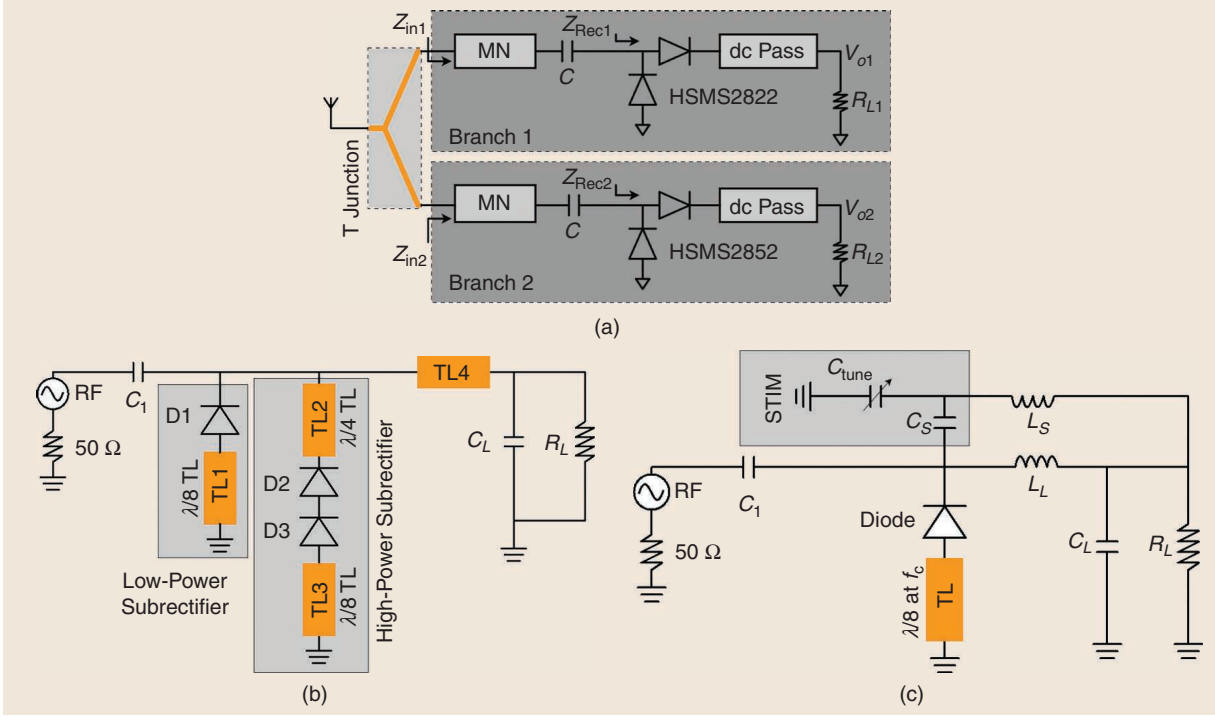

Figure 14. *Wide-dynamic-range rectifiers designed using (a) two subrectifiers with a T junction [57], (b) a PDDA [60], and (c) varactor-based STIM [61].*

It consists of a four-port RRC. Port 1 and port 3 were specified for antenna connection (or input power supply), while port 2 and port 4 were used to connect the rectifier circuit. The rectifier connected at port 2 was used to rectify the sum of the inputs, while the rectifier connected at port 4 was used to rectify the difference among the inputs. The impedances seen from port 2 and port 4 are $Z_{in2,0}$ and $Z_{in4,0}$ at $\Delta\varphi = 0°$ and $Z_{in2,180}$ and $Z_{in4,180}$ at $\Delta\varphi = 180°$. At $\Delta\varphi = 0°$, all energy flows toward port 2, and $Z_{in2,0}$ is the input impedance with

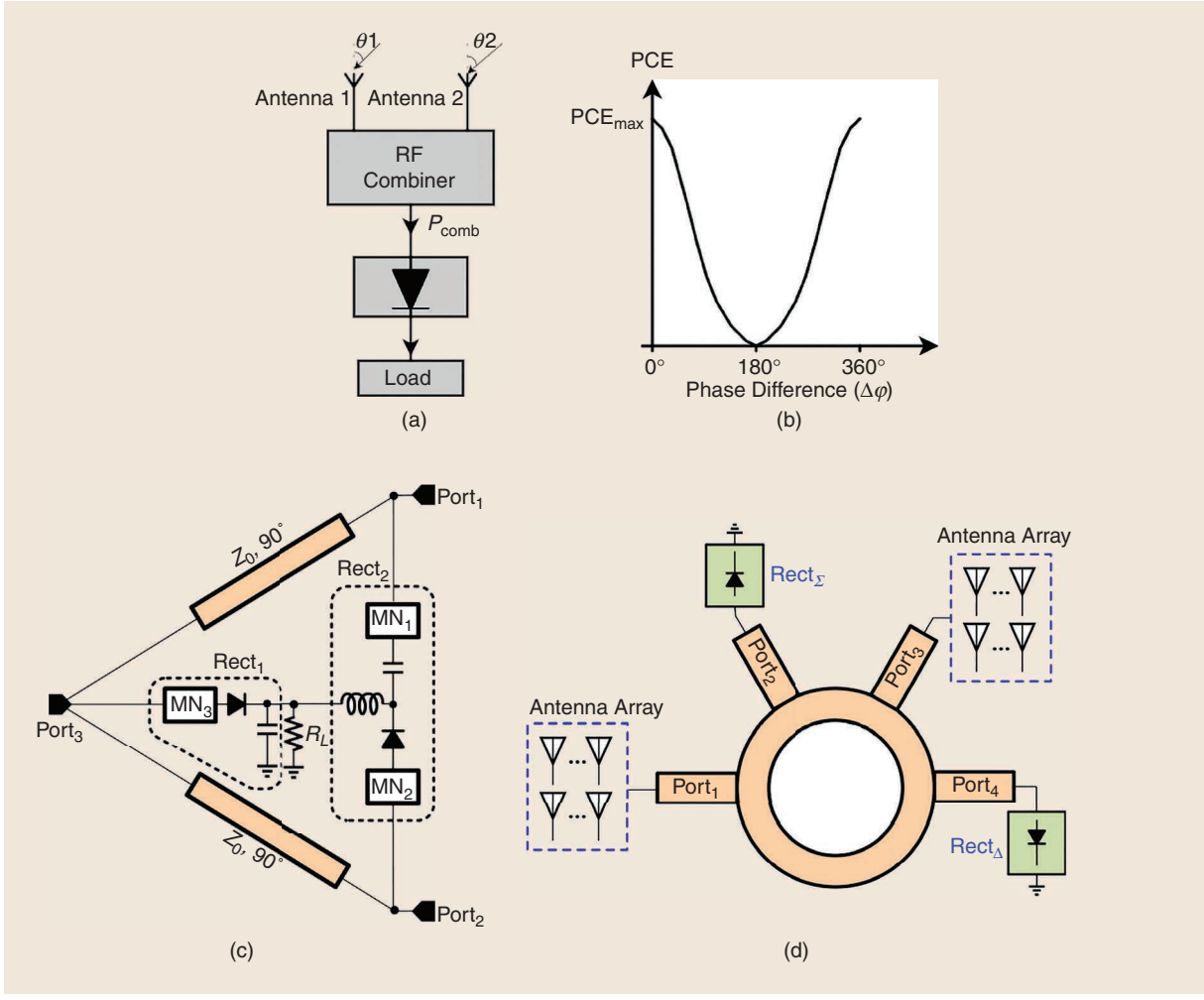

Figure 15. *(a) The RF-combining rectenna array. (b) The efficiency variation versus the phase difference. (c) A rectifier with a wide incident angle of incoming waves based on a Wilkinson power combiner. (d) A rectifier with a wide incident angle of incoming waves based on a rat race coupler [65].*

TABLE 5. The requirements of rectifiers in different scenarios.

Scenario Number	Scenario	Requirements
1 [17]	High dedicated power (P_H)	A rectifier using a Schottky diode having a high breakdown voltage and a low load that satisfy (7) and $P_H \le P_{oMax}$
2 [3]	Low ambient power (P_L)	A rectifier using a low-threshold Schottky diode
3 [40], [41]	Multiple ambient sources	A multiband rectifier or BBR using a multiband or broadband MN to improve captured power
4 [57]	A source having unstable power levels	A wide dynamic rectifier using a combination of multiple subrectifiers, each optimized for different input power levels
5 [65]	Low ambient power and an antenna array with an RF power combiner to enhance captured power	A rectifier that is insensitive or less sensitive to the incident angle of incoming waves by using a WPC, RRC, and so on

the highest power, while $Z_{in4,0}$ is the input impedance with the lowest power. At $\Delta\varphi = 180°$, all energy flows toward port 4, and $Z_{in2,180} = Z_{in4,0}$, and $Z_{in4,180} = Z_{in2,0}$. This means automatic impedance matching occurs, which ensures less deviation in the PCE for a wide range of $\Delta\varphi$.

PCE Improvement Techniques

The efficiency of RFEH/WPT systems primarily relies on the PCE of the rectifier circuit. Hence, to improve RFEH/WPT system performance, a highly efficient rectifier is needed. The efficiency of the rectifier can be calculated as a ratio of the output dc power (P_{outDC}) and RF power delivered to the rectifier ($P_{inRectifier}$), as shown in (8), where V_{outDC}, P_{inRF}, and $P_{Reflected}$ are the output dc voltage across the load, input RF power, and reflected power at the input of the rectifier, respectively. The performance of the rectifier is also improved theoretically with a perfect MN, as the efficiency depends on the input power fed to the rectifier. The nonlinear Schottky barrier diode (which is the key component of a rectifying circuit) produces harmonic signals during rectification, as in (5). As a result, the energy of the harmonic components could be lost. However, through trapping and rerectification, these harmonics produce more output power:

$$PCE = \frac{P_{outDC}}{P_{inRectifier}} = \frac{\frac{V_{outDC}^2}{R_L}}{P_{inRF} - P_{Reflected}}. \quad (8)$$

An HTN is one way to eliminate harmonic power dissipations. A class F HTN produces high-impedance third harmonics and low-impedance second harmonics [19], whereas an inverse class F HTN produces high-impedance second harmonics and low-impedance third harmonics [66]. In [67], both a class F and an inverse class F rectifier were characterized and compared. An inverse class F rectifier shows better efficiency due to less power loss. In [68], a class C and inverse class F HTN were utilized to improve the efficiency of a rectifier. In [69], waveform optimization was shown to improve the PCE of a rectifier based on the pulse-modulated signal. The authors showed that an RF pulse signal with a high peak-to-average-power ratio achieved better performance compared to a one-tone signal in a well-matched rectifier. In [70], the harmonic recycling concept was introduced to the recycling and rectification of harmonic components that enhance the rectifier PCE. In [58], the PCE was improved by utilizing a low-power subrectifier to collect and recycle the reflected power of the main subrectifier dealing with high power. This method also reduces the sensitivity of the rectifier to input power fluctuations (see Table 5).

The performance of the rectifier is also improved theoretically with a perfect MN, as the efficiency depends on the input power fed to the rectifier.

Conclusion

This article discussed, in detail, the current state of research into rectifier circuit designs for RFEH/WPT applications. PCE, bandwidth, and the dynamic operable range are the measures of rectifier performance. Various types of MNs have been utilized to enhance rectifier performance. To enhance understanding, rectifiers have been classified and discussed based upon operating conditions. Below 1 GHz, most of the designs focus on CMOS implementations, and above 1 GHz, Schottky diodes are preferred for designing rectifiers. Furthermore, efforts to extend the operating input power range, operating load range, and operating frequency range of rectifiers were also discussed. Hence, the authors' recommendations are as follows:

1) A Schottky diode with a low threshold voltage is best for low-power rectifier design.
2) A Schottky diode with a high breakdown voltage is best for high-power rectifier design.
3) Multiband rectifiers and BBRs are better when the goal is to increase the amount of collected power.
4) A combination of multiple subrectifiers, each optimized for a different input power level, is better when the goal is to extend the operable input power range and minimize the effect of changes in the input power level.
5) A rectifier that is insensitive or less sensitive to the incident angle of incoming waves is better for situations where an antenna array using an RF power combiner is used to enhance the captured power.

Acknowledgment

This work was supported by the Science and Engineering Research Board, Government of India, under the Visiting Advanced Joint Research Faculty Scheme (grant VJR/2019/000009, dated 22 July 2020).

References

[1] D. Surender, T. Khan, F. A. Talukdar, and Y. M. M. Antar, "Rectenna design and development strategies for wireless applications: A review," *IEEE Antennas Propag. Mag.*, early access, Aug. 12, 2021, doi: 10.1109/MAP.2021.3099722.

[2] A. Costanzo and D. Masotti, "Energizing 5G: Near- and far-field wireless energy and data trantransfer as an enabling technology for the 5G IoT," *IEEE Microw. Mag.*, vol. 18, no. 3, pp. 125–136, May 2017, doi: 10.1109/MMM.2017.2664001.

[3] M. Zeng, A. S. Andrenko, X. Liu, Z. Li, and H. Tan, "A compact fractal loop rectenna for RF energy harvesting," *IEEE Antennas*

Wireless Propag. Lett., vol. 16, pp. 2424–2427, Jul. 2017, doi: 10.1109/LAWP.2017.2722460.

[4] C. R. Valenta and G. D. Durgin, "Harvesting wireless power: survey of energy-harvester conversion efficiency in far-field, wireless power transfer systems," *IEEE Microw. Mag.*, vol. 15, no. 4, pp. 108–120, Jun. 2014, doi: 10.1109/MMM.2014.2309499.

[5] A. Collado, S. N. Daskalakis, K. Niotaki, R. Martinez, F. Bolos, and A. Georgiadis, "Rectifier design challenges for RF wireless power transfer and energy harvesting systems," *Radioengineering*, vol. 26, no. 2, pp. 411–417, 2017, doi: 10.13164/re.2017.0411.

[6] M. A. Halimi, T. Khan, M. Palandoken, A. A. Kishk, and Y. M. M. Antar, "Rectifier design challenges for WEH/WPT systems: Broadening bandwidth and extending input power range," *IEEE Microw. Mag.*, to be published.

[7] Y. Zhou, '"Contribution to electromagnetic energy harvesting for wireless autonomous devices," Ph.D. dissertation, Eng. Sci., De Nantes Univ., Nantes, France, 2013.

[8] S. A. Rotenberg, S. K. Podilchak, P. D. H. Re, C. Mateo-Segura, G. Goussetis, and J. Lee, "Efficient rectifier for wireless power transmission systems," *IEEE Trans Microw. Theory Techn.*, vol. 68, no. 5, pp. 1921–1932, May 2020, doi: 10.1109/TMTT.2020.2968055.

[9] C. Song, Y. Huang, P. Carter, J. Zhou, S. D. Joseph, and G. Li, "Novel compact and broadband frequency-selectable rectennas for a wide input-power and load impedance range," *IEEE Trans. Antennas Propag.*, vol. 66, no. 7, pp. 3306–3316, Jul. 2018, doi: 10.1109/TAP.2018.2826568.

[10] K. Kotani, A. Sasaki, and T. Ito, "High-efficiency differential-drive CMOS rectifier for UHF RFIDs," *IEEE J. Solid-State Circuits*, vol. 44, no. 11, pp. 3011–3018, Nov. 2009, doi: 10.1109/JSSC.2009.2028955.

[11] Y. Lu et al., "A wide input range dual-path CMOS rectifier for RF energy harvesting," *IEEE Trans. Circuits Syst., II, Exp. Briefs*, vol. 64, no. 2, pp. 166–170, Feb. 2017, doi: 10.1109/TCSII.2016.2554778.

[12] A. S. Almansouri, M. H. Ouda, and K. N. Salama, "A CMOS RF-to-DC power converter with 86% efficiency and –19.2-dBm sensitivity," *IEEE Trans. Microw. Theory Techn.*, vol. 66, no. 5, pp. 2409–2415, May 2018, doi: 10.1109/TMTT.2017.2785251.

[13] J. Guo, H. Zhang, and X. Zhu, "Theoretical analysis of RF-DC conversion efficiency for class-F rectifiers," *IEEE Trans. Microw. Theory Techn.*, vol. 62, no. 4, pp. 977–985, Apr. 2014, doi: 10.1109/TMTT.2014.2298368.

[14] T. Hu, M. Huang, Y. Lu, X. Y. Zhang, F. Maloberti, and R. P. Martins, "A 2.4-GHz CMOS differential class-DE rectifier with coupled inductors," *IEEE Trans. Power Electron.*, vol. 36, no. 9, pp. 9864–9875, Sep. 2021, doi: 10.1109/TPEL.2021.3061703.

[15] F. Zhao, D. Inserra, G. Gao, Y. Huang, J. Li, and G. Wen, "High-efficiency microwave rectifier with coupled transmission line for low-power energy harvesting and wireless power transmission," *IEEE Trans. Microw. Theory Techn.*, vol. 69, no. 1, pp. 916–925, Jan. 2021, doi: 10.1109/TMTT.2020.3027011.

[16] C. Liu, F. Tan, H. Zhang, and Q. He, "A novel single-diode microwave rectifier with a series band-stop structure," *IEEE Trans. Microw. Theory Techn.*, vol. 65, no. 2, pp. 600–606, Feb. 2017, doi: 10.1109/TMTT.2016.2626286.

[17] C. Wang, B. Yang, and N. Shinohara, "Study and design of a 2.45-GHz rectifier achieving 91% efficiency at 5-W input power," *IEEE Microw. Wireless Compon. Lett.*, vol. 31, no. 1, pp. 76–79, Jan. 2021, doi: 10.1109/LMWC.2020.3032574.

[18] H. Xiao, H. Zhang, W. Song, J. Wang, W. Chen, and M. Lu, "A high-input power rectifier circuit for 2.45-GHz microwave wireless power transmission," *IEEE Trans. Ind. Electron.*, vol. 69, no. 3, pp. 2896–2903, Mar. 2022, doi: 10.1109/TIE.2021.3063971.

[19] F. Zhao, Z. Li, G. Wen, J. Li, D. Inserra, and Y. Huang, "A compact high-efficiency watt-level microwave rectifier with a novel harmonic termination network," *IEEE Microw. Wireless Compon. Lett.*, vol. 29, no. 6, pp. 418–420, Jun. 2019, doi: 10.1109/LMWC.2019.2913782.

[20] M. A. Halimi, D. Surender, and T. Khan, "Design of a 2.45 GHz operated rectifier with 81.5% PCE at 13 dBm input power for RFEH/WPT applications," in *Proc. 2021 IEEE Indian Conf. Antennas Propag. (InCAP)*, Jaipur, India, pp. 981–983, doi: 10.1109/InCAP52216.2021.9726346.

[21] C. Wang, N. Shinohara, and T. Mitani, "Study on 5.8 GHz band rectenna rectifying circuit for internal wireless system of satellite," in *Proc. 2016 IEEE Wireless Power Transfer Conf. (WPTC)*, Aveiro, pp. 1–4, doi: 10.1109/WPT.2016.7498852.

[22] C. Wang, N. Shinohara, and T. Mitani, "Study on 5.8-GHz single-stage charge pump rectifier for internal wireless system of satellite," *IEEE Trans. Microw. Theory Techn.*, vol. 65, no. 4, pp. 1058–1065, Apr. 2017, doi: 10.1109/TMTT.2017.2672552.

[23] D. Surender, M. A. Halimi, T. Khan, F. A. Talukdar, and Y. M. M. Antar, "A 90° twisted quarter-sectored compact and circularly polarized DR-rectenna for RF energy harvesting applications," *IEEE Antennas Wireless Propag. Lett.*, vol. 21, no. 6, pp. 1139–1143, Jun. 2022, doi: 10.1109/LAWP.2022.3159482.

[24] N. Sakai, K. Noguchi, and K. Itoh, "A 5.8-GHz band highly efficient 1-W rectenna with short-stub-connected high-impedance dipole antenna," *IEEE Trans. Microw. Theory Techn.*, vol. 69, no. 7, pp. 3558–3566, Jul. 2021, doi: 10.1109/TMTT.2021.3074592.

[25] U. Olgun, C. Chen, and J. L. Volakis, "Investigation of rectenna array configurations for enhanced RF power harvesting," *IEEE Antennas Wireless Propag. Lett.*, vol. 10, pp. 262–265, Apr. 2011, doi: 10.1109/LAWP.2011.2136371.

[26] N. Tung, "Multi-band ambient RF energy harvesting rectifier for autonomous Wireless Sensor networks," in *Proc. 2016 IEEE Region 10 Conf. (TENCON)*, Singapore, pp. 3736–3739, doi: 10.1109/TENCON.2016.7848758.

[27] M. A. Halimi, T. Khan, S. K. Koul, and S. R. Rengarajan, "A dual-band rectifier using half-wave transmission line matching for 5G and Wi-Fi bands RFEH/MPT applications," *IEEE Microw. Wireless Compon. Lett.*, early access, Aug. 16, 2022, doi: 10.1109/LMWC.2022.3197590.

[28] L. Guo, X. Li, P. Chu, and K. Wu, "Accurately modeling zero-bias diode-based RF power harvesters with wide adaptability to frequency and power," *IEEE Trans. Circuits Syst. I, Reg. Papers*, vol. 68, no. 12, pp. 5194–5205, Dec. 2021, doi: 10.1109/TCSI.2021.3112672.

[29] S. Li, F. Cheng, C. Gu, S. Yu, and K. Huang, "Efficient dual-band rectifier using stepped impedance stub matching network for wireless energy harvesting," *IEEE Microw. Wireless Compon. Lett.*, vol. 31, no. 7, pp. 921–924, Jul. 2021, doi: 10.1109/LMWC.2021.3078546.

[30] J. Liu, M. Huang, and Z. Du, "Design of compact dual-band rf rectifiers for wireless power transfer and energy harvesting," *IEEE Access*, vol. 8, pp. 184,901–184,908, Oct. 2020, doi: 10.1109/ACCESS.2020.3029603.

[31] A. Quddious, S. Zahid, F. A. Tahir, M. A. Antoniades, P. Vryonides, and S. Nikolaou, "Dual-band compact rectenna for UHF and ISM wireless power transfer systems," *IEEE Trans. Antennas Propag.*, vol. 69, no. 4, pp. 2392–2397, Apr. 2021, doi: 10.1109/TAP.2020.3025299.

[32] M. A. Halimi, D. Surender, T. Khan, F. A. Talukdar, S. K. Koul, and Y. M. M. Antar, "A multistepped transmission line matching strategy based triple-band rectifier for RFEH/WPT applications," *IEEE Microw. Wireless Compon. Lett.*, vol. 32, no. 8, pp. 1007–1010, Aug. 2022, doi: 10.1109/LMWC.2022.3162633.

[33] A. Riaz, S. Zakir, M. M. Farooq, M. Awais, and W. T. Khan, "A triband rectifier toward millimeter-wave frequencies for energy harvesting and wireless power-transfer applications," *IEEE Microw. Wireless Compon. Lett.*, vol. 31, no. 2, pp. 192–195, Feb. 2021, doi: 10.1109/LMWC.2020.3037137.

[34] J. Liu and X. Y. Zhang, "Compact triple-band rectifier for ambient RF energy harvesting application," *IEEE Access*, vol. 6, pp. 19,018–19,024, Mar. 2018, doi: 10.1109/ACCESS.2018.2820143.

[35] Z. Li, M. Zeng, and H. Z. Tan, "A multi-band rectifier with modified hybrid junction for RF energy harvesting," *Microw. Opt. Technol. Lett.*, vol. 60, no. 4, pp. 817–821, 2018, doi: 10.1002/mop.31057.

[36] M. Q. Dinh and M. Thuy Le, "Triplexer-based multiband rectenna for RF energy harvesting from 3G/4G and Wi-Fi," *IEEE Microw. Wireless Compon. Lett.*, vol. 31, no. 9, pp. 1094–1097, Sep. 2021, doi: 10.1109/LMWC.2021.3095074.

[37] C. Hsu, S. Lin, and Z. Tsai, "Quadband rectifier using resonant matching networks for enhanced harvesting capability," *IEEE Microw. Wireless Compon. Lett.*, vol. 27, no. 7, pp. 669–671, Jul. 2017, doi: 10.1109/LMWC.2017.2711578.

[38] V. Kuhn, C. Lahuec, F. Seguin, and C. Person, "A multi-band stacked RF energy harvester with RF-to-DC efficiency up to 84%," *IEEE Trans. Microw. Theory Techn.*, vol. 63, no. 5, pp. 1768–1778, May 2015, doi: 10.1109/TMTT.2015.2416233.

[39] J. Lu, X. Yang, H. Mei, and C. Tan, "A four-band rectifier with adaptive power for electromagnetic energy harvesting," *IEEE Microw. Wireless Compon. Lett.*, vol. 26, no. 10, pp. 819–821, Oct. 2016, doi: 10.1109/LMWC.2016.2601294.

[40] C. Song, et al. "A novel six-band dual cp rectenna using improved impedance matching technique for ambient rf energy harvesting," *IEEE Trans. Antennas Propag.*, vol. 64, no. 7, pp. 3160–3171, Jul. 2016, doi: 10.1109/TAP.2016.2565697.

[41] W. Liu, K. Huang, T. Wang, J. Hou, and Z. Zhang, "Broadband high-efficiency RF rectifier with a cross-shaped match stub of two one-eighth-wavelength transmission lines," *IEEE Microw. Wireless Compon. Lett.*, vol. 31, no. 10, pp. 1170–1173, Oct. 2021, doi: 10.1109/LMWC.2021.3082930.

[42] S. Yu, F. Cheng, C. Gu, C. Wang, and K. Huang, "Compact and efficient broadband rectifier using T-type matching network," *IEEE Microw. Wireless Compon. Lett.*, vol. 32, no. 6, pp. 587–590, Jun. 2022, doi: 10.1109/LMWC.2022.3146883.

[43] W. Liu, K. Huang, T. Wang, J. Hou, and Z. Zhang, "A compact high-efficiency RF rectifier with widen bandwidth," *IEEE Microw. Wireless Compon. Lett.*, vol. 32, no. 1, pp. 84–87, Jan. 2022, doi: 10.1109/LMWC.2021.3115106.

[44] J. Kimionis, A. Collado, M. M. Tentzeris, and A. Georgiadis, "Octave and decade printed UWB rectifiers based on non-uniform transmission lines for energy harvesting," *IEEE Trans. Microw. Theory Techn.*, vol. 65, no. 11, pp. 4326–4334, Nov. 2017, doi: 10.1109/TMTT.2017.2697851.

[45] M. M. Mansour and H. Kanaya, "Compact and broadband RF rectifier with 1.5 octave bandwidth based on a simple pair of L-section matching network," *IEEE Microw. Wireless Compon. Lett.*, vol. 28, no. 4, pp. 335–337, Apr. 2018, doi: 10.1109/LMWC.2018.2808419.

[46] M. M. Mansour and H. Kanaya, "High-efficient broadband CPW RF rectifier for wireless energy harvesting," *IEEE Microw. Wireless Compon. Lett.*, vol. 29, no. 4, pp. 288–290, Apr. 2019, doi: 10.1109/LMWC.2019.2902461.

[47] Y. L. Lin, X. Y. Zhang, Z. X. Du, and Q. W. Lin, "High-efficiency microwave rectifier with extended operating bandwidth," *IEEE Trans. Circuits Syst., II, Exp. Briefs*, vol. 65, no. 7, pp. 819–823, Jul. 2018, doi: 10.1109/TCSII.2017.2716538.

[48] B. Zeng, S. Zheng, B. K. W. Leung, and M. Xia, "An ultrawideband high-efficiency rectifier based on harmonic feedback topology," *IEEE Trans. Ind. Electron.*, vol. 69, no. 8, pp. 7974–7983, Aug. 2022, doi: 10.1109/TIE.2021.3105989.

[49] P. Wu et al., "Compact high-efficiency broadband rectifier with multi-stage-transmission-line matching," *IEEE Trans. Circuits Syst., II, Exp. Briefs*, vol. 66, no. 8, pp. 1316–1320, Aug. 2019, doi: 10.1109/TCSII.2018.2886432.

[50] P. Wu, S. Y. Huang, W. Zhou, and C. Liu, "One octave bandwidth rectifier with a frequency selective diode array," *IEEE Microw. Wireless Compon. Lett.*, vol. 28, no. 11, pp. 1008–1010, Nov. 2018, doi: 10.1109/LMWC.2018.2869281.

[51] X. Gu, P. Burasa, S. Hemour, and K. Wu, "Recycling ambient RF energy: Far-field wireless power transfer and harmonic backscattering," *IEEE Microw. Mag.*, vol. 22, no. 9, pp. 60–78, Sep. 2021, doi: 10.1109/MMM.2021.3086335.

[52] S. Hemour et al., "Towards low-power high-efficiency RF and microwave energy harvesting," *IEEE Trans. Microw. Theory Techn.*, vol. 62, no. 4, pp. 965–976, Apr. 2014, doi: 10.1109/TMTT.2014.2305134.

[53] D. Masotti, A. Costanzo, P. Francia, M. Filippi, and A. Romani, "A load-modulated rectifier for RF micropower harvesting with start-up strategies," *IEEE Trans. Microw. Theory Techn.*, vol. 62, no. 4, pp. 994–1004, Apr. 2014, doi: 10.1109/TMTT.2014.2304703.

[54] J. Liu, X. Y. Zhang, and Q. Xue, "Dual-band transmission-line resistance compression network and its application to rectifiers," *IEEE Trans. Circuits Syst. I, Reg. Papers*, vol. 66, no. 1, pp. 119–132, Jan. 2019, doi: 10.1109/TCSI.2018.2852321.

[55] Z. Du and X. Y. Zhang, "High-efficiency single- and dual-band rectifiers using a complex impedance compression network for wireless power transfer," *IEEE Trans. Ind. Electron.*, vol. 65, no. 6, pp. 5012–5022, Jun. 2018, doi: 10.1109/TIE.2017.2772203.

[56] Y. Y. Xiao, J. Ou, Z. Du, X. Y. Zhang, W. Che, and Q. Xue, "Compact microwave rectifier with wide input power dynamic range based on integrated impedance compression network," *IEEE Access*, vol. 7, pp. 151,878–151,887, Oct. 2019, doi: 10.1109/ACCESS.2019.2948114.

[57] M. Huang et al., "Single- and dual-band RF rectifiers with extended input power range using automatic impedance transforming," *IEEE Trans. Microw. Theory Techn.*, vol. 67, no. 5, pp. 1974–1984, May 2019, doi: 10.1109/TMTT.2019.2901443.

[58] Y. Y. Xiao, Z. Du, and X. Y. Zhang, "High-efficiency rectifier with wide input power range based on power recycling," *IEEE Trans. Circuits Syst., II, Exp. Briefs*, vol. 65, no. 6, pp. 744–748, Jun. 2018, doi: 10.1109/TCSII.2018.2794551.

[59] P. Wu, Y. Chen, W. Zhou, Z. H. Ren, and S. Y. Huang, "A wide dynamic range rectifier array based on automatic input power distribution technique," *IEEE Microw. Wireless Compon. Lett.*, vol. 30, no. 4, pp. 437–440, Apr. 2020, doi: 10.1109/LMWC.2020.2972727.

[60] Z. He, J. Lan, and C. Liu, "Compact rectifiers with ultra-wide input power range based on nonlinear impedance characteristics of Schottky diodes," *IEEE Trans. Power Electron.*, vol. 36, no. 7, pp. 7407–7411, Jul. 2021, doi: 10.1109/TPEL.2020.3046083.

[61] P. Wu et al., "High-efficient rectifier with extended input power range based on self-tuning impedance matching," *IEEE Microw. Wireless Compon. Lett.*, vol. 28, no. 12, pp. 1116–1118, Dec. 2018, doi: 10.1109/LMWC.2018.2876773.

[62] T. Ngo, A. Huang, and Y. Guo, "Analysis and design of a reconfigurable rectifier circuit for wireless power transfer," *IEEE Trans. Ind. Electron.*, vol. 66, no. 9, pp. 7089–7098, Sep. 2019, doi: 10.1109/TIE.2018.2875638.

[63] Z. Liu, Z. Zhong, and Y. X. Guo, "Enhanced dual-band ambient RF energy harvesting with ultra-wide power range," *IEEE Microw. Wireless Compon. Lett*, vol. 25, no. 9, pp. 630–632, Sep. 2015, doi: 10.1109/LMWC.2015.2451397.

[64] S. N. Daskalakis, A. Georgiadis, G. Goussetis, and M. M. Tentzeris, "A rectifier circuit insensitive to the angle of incidence of incoming waves based on a Wilkinson power combiner," *IEEE Trans. Microw. Theory Techn.*, vol. 67, no. 7, pp. 3210–3218, Jul. 2019, doi: 10.1109/TMTT.2019.2912192.

[65] J. Liu, M. Huang, Y. Lu, and R. P. Martins, "RF rectifiers with wide incident angle of incoming waves based on rat-race couplers," *IEEE Trans. Microw. Theory Techn.*, vol. 70, no. 3, pp. 1983–1993, Mar. 2022, doi: 10.1109/TMTT.2021.3132331.

[66] F. Zhao, D. Inserra, G. Wen, J. Li, and Y. Huang, "A high-efficiency inverse class-F microwave rectifier for wireless power transmission," *IEEE Microw. Wireless Compon. Lett.*, vol. 29, no. 11, pp. 725–728, Nov. 2019, doi: 10.1109/LMWC.2019.2944525.

[67] S. Abbasian and T. Johnson, "Power-efficiency characteristics of class-F and inverse class-F synchronous rectifiers," *IEEE Trans. Microw. Theory Techn.*, vol. 64, no. 12, pp. 4740–4751, Dec. 2016, doi: 10.1109/TMTT.2016.2623708.

[68] M. Roberg, T. Reveyrand, I. Ramos, E. A. Falkenstein, and Z. Popovic, "High-efficiency harmonically terminated diode and transistor rectifiers," *IEEE Trans. Microw. Theory Techn.*, vol. 60, no. 12, pp. 4043–4052, Dec. 2012, doi: 10.1109/TMTT.2012.2222919.

[69] V.D. Pham, H. Takhedmit, and L. Cirio, "Waveform optimization for efficiency improvement of traditional RF-to-dc rectifiers without input matching network," in *Proc. 2020 14th Eur. Conf. Antennas Propag. (EuCAP)*, Copenhagen, Denmark, pp. 1–5, doi: 10.23919/EuCAP48036.2020.9135994.

[70] T. Ngo and Y. Guo, "Harmonic-recycling rectifier for high-efficiency far-field wireless power transfer," *IEEE Trans. Circuits Syst., II, Exp. Briefs*, vol. 67, no. 4, pp. 770–774, Apr. 2020, doi: 10.1109/TCSII.2019.2923838.